Zigzag transition of finite dust clusters

André Melzer
Institut für Physik, Ernst-Moritz-Arndt-Universität Greifswald, 17487 Greifswald, Germany
(Received 22 February 2006; published 23 May 2006)

Experiments on the zigzag transition of finite dust clusters are presented. There, microspheres have been confined in an anisotropic trap in the sheath of a radio-frequency discharge plasma. Transitions of the clusters from a linear chain into a zigzag configuration are observed by increasing the particle number in the chain or by variation of the anisotropy of the confinement. The equilibrium configurations of the finite clusters, as well as the dynamical properties and the stability behavior near the transition have been investigated from a normal mode analysis. Furthermore, the longitudinal and transverse dispersion of the normal modes in the one-dimensional (1D) chain has been derived.

DOI: 10.1103/PhysRevE.73.056404 PACS number(s): 52.27.Lw, 36.40.Ei, 52.35.−g

I. INTRODUCTION

There is an enormous interest in the static and dynamic behavior of Coulomb clusters. They consist of a finite number of charged particles in an external confinement. Such Coulomb clusters are found, to name a few, as electrons or ions in Paul or Penning traps [1], ions in storage rings [2], electron droplets on liquid helium [3], or polymer particles in colloidal suspensions [4].

In this respect, dusty plasmas provide an ideal and versatile system to study finite charged-particle systems. Dusty plasmas consist of solid particles immersed in a plasma environment. For the investigation of finite Coulomb clusters usually plastic microspheres of 1–10 micrometer diameter are trapped in a plasma discharge. Due to the collection of plasma electrons and ions the microspheres attain high negative charges of the order of 10^4 elementary charges. Because of this high particle charge the microspheres form strongly coupled systems even at room temperature. Trapping in the discharge can be achieved by a force balance of various forces, like electric field force, gravity or thermophoresis [5]. In contrast to ions in traps, the particles in a dusty plasma do not interact by a pure Coulomb potential, but is shielded Debye-Hückel or Yukawa potential of the form

$$\phi(r) = \frac{Ze}{4\pi\epsilon_0 r} \exp\left(-\frac{r}{\lambda_D}\right), \tag{1}$$

where λ_D is the shielding length and Z is the particle charge. Nevertheless, to express the electrostatic nature of these systems, they are usually also referred to as "Coulomb clusters," although "Yukawa cluster" might be more appropriate.

Finite Coulomb (Yukawa) clusters in dusty plasmas have been investigated experimentally in various configurations. Clusters have been studied in two dimensions (2D) with isotropic confinement [6–9] in view of structure, rotational stability and normal modes. Linear [one-dimensional (1D)] systems have been explored by wave excitation and propagation [10] and their phonon spectrum has been analyzed in great detail see, e.g., Ref. [11]. Recently, isotropic three-dimensional (3D) clusters (so-called Coulomb balls) have been generated in the laboratory [12,13]. There, the onion-like shell structure and the properties of the confinement have been identified and measured [12,14]. However, transition between the various configurations have not been investigated so far.

Hence, in this paper, we present experiments on the transition from the strictly one-dimensional linear chain of particles to 2D structures in an anisotropic confinement. From simulations [15] it is known that a transition from a strict 1D to a 2D structure occurs via a zigzag transition at a critical value of the anisotropy. There the particles in the center of the chain, where the interparticle distance is smallest, are elongated from their chain position alternately in perpendicular (transverse) direction forming a zigzag pattern. Here, experiments on the zigzag transition by variation of the number of particles in a chain and by changing the anisotropy of the confinement will be presented. Their static and dynamic properties near the transition are described.

II. EXPERIMENTAL METHODS AND MODEL

The experiments have been performed in a parallel plate rf discharge (13.56 MHz at 5 W) in Argon at gas pressures between 2 and 10 Pa. Plastic microspheres (melamine formaldehyde) of 10.2 micron diameter (and a mass of $m=8.41\times10^{-13}$ kg) are dropped into the discharge. A rectangular barrier of 6 mm height and 5×40 mm^2 inner dimension is placed onto the lower electrode [see Fig. 1(a)]. The particles are trapped above the groove of the barrier by a force balance of electric field force and gravity. The barrier provides an anisotropic confinement for the particles in the horizontal plane. The particles are illuminated by a laser diode and the scattered light is recorded by a video camera at a frame rate of 50 fps with megapixel resolution.

The dust cluster is trapped in the potential well provided by the barrier on the electrode. The barrier distorts the electrostatic equipotential lines in the plasma sheath above the electrode and thus forms an anisotropic confinement since the size of the barrier in the y-direction is much larger than in the x-direction (Fig. 1). Consequently, the 3D potential well is cigar-shaped of the form

$$V(x,y,z) = \frac{1}{2}m(\omega_x^2 x^2 + \omega_y^2 y^2 + \omega_z^2 z^2)$$

where x,y are Cartesian coordinates in the horizontal plane and z denotes the vertical direction. The vertical confinement

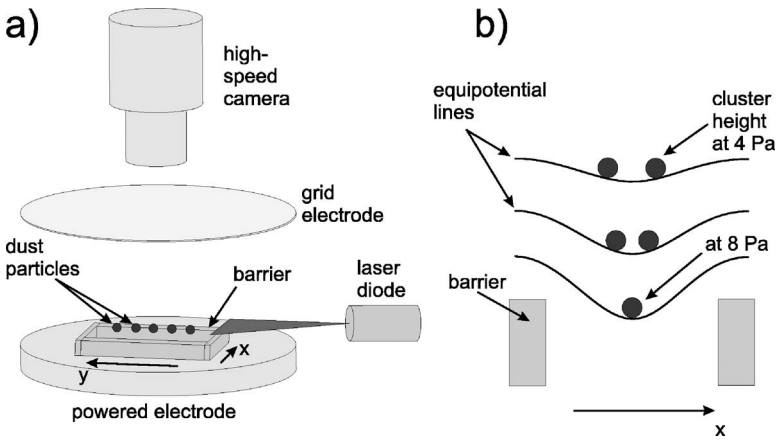

FIG. 1. (a) Scheme of the experimental setup. (b) Cross section through the barrier: Illustration of the equipotential lines and cluster height above the confining barrier.

is due to gravity and electric field force and is much stronger than the horizontal confinement [16] with high vertical resonance frequency $\omega_z \gg \omega_x, \omega_y$. Consequently, the motion of the microspheres is restricted to the x and y direction, only. Hence, the vertical direction will be ignored in the following discussions.

The total energy of N dust particles confined in the anisotropic horizontal confinement is then given by [17]

$$E = \frac{1}{2} m \omega_0^2 \sum_{i=1}^{N} (x_i^2 + \beta y_i^2) + \frac{Z^2 e^2}{4\pi\epsilon_0} \sum_{i>j}^{N} \frac{\exp(-r_{ij}/\lambda_D)}{r_{ij}}. \quad (2)$$

The first term is the potential energy in the confining well of the barrier, the second is the (screened) Coulomb energy between the particles. Here, we have chosen $\omega_0 = \omega_x$ and $\beta = \omega_y^2/\omega_x^2$ is the parameter of anisotropy. Due to the shape of the barrier $\omega_y < \omega_x$ and thus $\beta < 1$. Isotropic 2D confinement corresponds to $\beta = 1$. With $\beta \ll 1$ the confinement is anisotropic towards a 1D shape.

As mentioned above, the (screened) Coulomb interaction energy is characterized by the particle charge Z and the Debye screening length λ_D. Finally, x_i, y_i are the x, y position of particle i relative to the center of the confinement, respectively, and $r_{ij} = [(x_i - x_j)^2 + (y_i - y_j)^2]^{1/2}$ is the interparticle distance between particles i and j.

Using the normalization

$$r_0 = \left[\frac{Z^2 e^2}{4\pi\epsilon_0} \frac{2}{m\omega_0^2} \right]^{1/3} \text{and } E_0 = \left[\frac{m\omega_0^2}{2} \left(\frac{Z^2 e^2}{4\pi\epsilon_0} \right)^2 \right]^{1/3} \quad (3)$$

the total energy can be simply written as

$$E = \sum_{i=1}^{N} (x_i^2 + \beta y_i^2) + \sum_{i>j}^{N} \frac{\exp(-\kappa r_{ij})}{r_{ij}}, \quad (4)$$

where $\kappa = r_0/\lambda_D$ is the screening strength. One should note that the length scale r_0 is of the order of the interparticle distance.

When the confinement in x-direction is by far stronger than that in y (i.e., $\beta \ll 1$) the particles will arrange in a single linear chain (see Fig. 2). Diminishing the confinement strength ω_x (thus increasing β), the linear chain makes a transition into a zigzag arrangement at a critical anisotropy parameter β_c [15]. This critical parameter also depends on the number of trapped particles N. From a fit to numerical simulations, this critical parameter is found to scale as [17]

$$\beta_c = 3.23 N^{-1.82} \quad (5)$$

by Candido *et al.* (CRSP) for pure Coulomb interaction ($\kappa = 0$). Dubin and O'Neil (DN) have calculated the critical anisotropy parameter from the local density approximation as [1]

$$\beta_c = \frac{\ln(6N) + \gamma - 13/5}{0.591 N^2}. \quad (6)$$

Here, $\gamma = 0.577$ is Euler's constant. The DN expression for the critical β_c is reliable for large N, $N > 10$ say.

III. EXPERIMENTAL RESULTS

A. Static properties

In our experiments, the zigzag transition of the dust cluster is investigated by either variation of particle number N or by changing the anisotropy parameter β. Here, we start with the description of the variation of particle number. The experiments have been performed at fixed discharge parameters: The gas pressure was 3.9 Pa at a plasma power of 5 W.

Then, N particles have been dropped into the confinement of the barrier. All clusters between $N = 4$ and $N = 15$ plus $N = 18$ have been realized and recorded. For $N \leq 9$, the particles

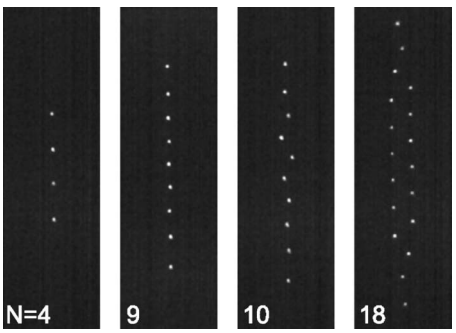

FIG. 2. Snapshots of the dust cluster for $N = 4$, 9, 10, and 18. The zigzag transition is observed for $N = 10$ particles. The size of each image corresponds to 2.8×9.1 mm^2.

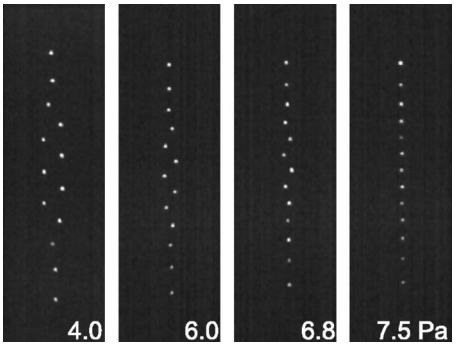

FIG. 3. Snapshots of the dust cluster with $N=13$ for $p=4.0$, 6.0, 6.8, and 7.5 Pa. The zigzag configuration is observed for $p<7.5$ Pa. The size of each image corresponds to 2.8×9.1 mm^2.

arrange in a strict 1D linear chain (see Fig. 2). At $N=10$, the transition into a zigzag pattern occurs. At $N=10$ only the central 3 particles show a perpendicular (transverse) elongation. With increased particle number ($N=18$), more and more particles are involved in the zigzag pattern. The general appearance of the clusters is very similar to the simulations [15].

This zigzag transition is easily understood: By adding more particles into the chain, the particles in the center of the confinement are more strongly compressed by the outer particles due to the confining potential ω_y. If the force on the central particles exceeds a certain threshold the particles deviate into the transverse direction. Then, the transverse confining force due to the potential ω_x is smaller than the compression of the N particles in the confinement ω_y and the (screened) Coulomb repulsion among the particles.

In our second experiment, the anisotropy of the confinement was changed. This was achieved by a variation of the gas pressure in the discharge between 4 and 8 Pa. At low gas pressure (4 Pa) the cluster is trapped relatively far above the barrier since the plasma sheath width is large at low gas pressure. At that height, the equipotential lines are only weakly bent by the barrier. This corresponds to a weak confinement ω_x (and thus to a relatively high $\beta=\omega_y/\omega_x$). In contrast, at higher gas pressure, the sheath width decreases, the cluster is confined closer to the electrode and, thus, closer to the barrier where the equipotential lines provide a deep trough with strong confinement ω_x (and small β). This behavior is illustrated in Fig. 1(b). Since the barrier is much more extended in the y-direction the influence of trapping height on ω_y is not as large as on ω_x.

Figure 3 shows the cluster configurations for different gas pressures. As expected, for low gas pressures $p<7.5$ Pa the cluster exhibits a zigzag pattern due to the weak confinement ω_x. Only at $p=7.5$ Pa a strict 1D linear chain is observed. This transition can be induced reversibly with gas pressure without noticeable hysteresis. At 6.8 Pa only the innermost 3 to 4 particles show the zigzag pattern, whereas at 4.0 Pa the largest part of the cluster is in zigzag configuration with much larger perpendicular elongation. This reflects the weaker confinement (and higher β) at lower gas pressure. The behavior is thus comparable to that with particle number variation.

A change of plasma power should also have an effect on the strength of the confining potential because of the change of the electron and ion density in the sheath. While some effect has been observed a clear transition between 1D and zigzag has not been found in the investigated parameter range.

B. Comparison to the model

For a detailed comparison of the experiment with the model the anisotropy parameter β has to be determined from the experiment. This has been done for the configurations that show a zigzag pattern, i.e., for $N\geqslant10$ at 3.9 Pa and for $p\leqslant6.8$ Pa at $N=13$. From the strict 1D chain that parameter has not been derived.

To determine β, we assume that the observed configuration is in equilibrium which means that for each particle the net force [due to (screened) Coulomb repulsion from the other particles and due to the confinement] is zero. We have calculated the force $F^i_{x,y}$ on the ith particle in x and y-direction by

$$F^i_x=-\frac{\partial E}{\partial x_i} \text{ and } F^i_y=-\frac{\partial E}{\partial y_i}$$

where the energy in the form

$$E/E_0=\sum_{i=1}^{N}\frac{1}{r_0^2}(x_i^2+\beta y_i^2)+\sum_{i>j}^{N}\frac{r_0}{r_{ij}}\exp(-\kappa r_{ij}),$$

is used. The forces were obtained using the measured coordinates x_i and y_i of the cluster with a chosen value of $\kappa=0,\ldots,4$. The energy includes the scaling parameter r_0 which is *a priori* undetermined due to the unknown values of the particle charge Z and the confining potential ω_0^2. The parameter E_0 can be ignored here because the absolute value of the energy and the force is not required.

Now, in a first step the length scaling r_0 is found from the condition that the forces F^i_x on all particles in x-direction should vanish. The forces F^i_x are used in this first step since they do not contain the second unknown β. Numerically, r_0 is derived as the value that minimizes $\Sigma_i^N|F^i_x|$. Depending on κ, r_0 lies in the range between 370 and 900 μm which is of the order of the interparticle distance.

Having now determined r_0, the anisotropy parameter β is found in a similar manner using the forces in y-direction. It is found from the minimum of $\Sigma_i^N|F^i_y|$ using the previously derived value of r_0. The obtained values of r_0 and β are compiled in Tables I and II.

In the experiment with variation of particle number the obtained values of r_0 and β are found to be independent of N (within statistical limits) as one would expect. Hence, Table I gives the mean values and the root-mean-square deviation of these parameters. These values are also used in the subsequent analysis of the strict 1D chains with $N\leqslant9$. Of course, the values depend on the chosen screening strength κ since that determines the electrostatic forces between the particles and, consequently, the necessary strength of the confinement.

In the experiment with variation of gas pressure (Table II), the anisotropy parameter β is found to decrease continu-

TABLE I. Scaling parameter r_0 and anisotropy parameter β determined from the observed configurations with $N \geqslant 10$. The given quantities are the mean values and root-mean-square deviations.

	$\kappa=0$	$\kappa=1$	$\kappa=2$	$\kappa=3$	$\kappa=4$
r_0/μm	505±10	581±10	685±9	775±18	877±23
$\beta/10^{-2}$	5.3±0.5	2.8±0.3	2.3±0.3	2.0±0.5	2.0±0.6

ously, indicating a stronger transverse confinement. This exactly reflects the observations from the experiment.

The obtained anisotropy parameters are compared to the model predictions of CRSP [17] and DN [1] in Fig. 4. Using the experimental values of β from the particle number experiment and noting that the zigzag transition in this experiment occurs between 9 and 10 particles, full agreement is obtained with the model of CRSP with a chosen value of $\kappa=0$. As in the experiment, CRSP predicts the transition precisely between 9 and 10 particles. The model of DN is in agreement for $\kappa \approx 0.5$. According to the DN model the zigzag transition would occur between 7 and 8 particles using the β-value at $\kappa=0$, between 9 and 10 particles at $\kappa=0.5$, and between 11 and 12 particles at $\kappa=1$.

The pressure variation experiment with $N=13$ yields a critical anisotropy parameter that is again very close to the model of CRSP at $\kappa=0$. The experiment is again close to the model of DN when κ is chosen near 0.5.

Summarizing, very close quantitative agreement between the experiment and the models is found in the range of screening strengths from $\kappa=0$ to 1. Very similar values of the screening strength have been obtained in previous experiments on 1D and 2D clusters [8,11]. Thus, the static properties are thus very well described by the models.

C. Dynamical properties and stability

We will now discuss the dynamical behavior and the stability of the dust clusters near the zigzag transition.

The dynamical properties and the stability of dust clusters are usually analyzed in terms of the normal modes of the system. This technique has been used to determine the mode spectrum of extended 2D crystals [18], isotropic 2D dust clusters [8], or long 1D chains [11]. The application of this method to finite dust clusters is described in detail in Ref. [8] and will only be briefly summarized here.

First, the normal modes of a finite cluster are the eigenvalues and eigenvectors of the dynamical matrix [19]

$$E_{\alpha,\alpha',ij} = \frac{\partial^2 E}{\partial r_{\alpha,i} \partial r_{\alpha',j}},$$

where $r_{\alpha,i}$ denotes the x or y coordinate of the ith particle ($\alpha, \alpha' = x$ or y). The eigenvectors of the dynamical matrix describe the mode oscillation patterns of the cluster and the eigenvalues are the oscillation frequencies of the respective modes. Experimentally, the normal mode spectra are obtained as the spectral power density of mode number $\ell = 1, \ldots, 2N$ by

$$S_\ell(\omega) = \frac{2}{T} \left| \int_0^T v_\ell(t) e^{i\omega t} \right|^2.$$

Here, $v_\ell(t) = \sum_{i=1}^{N} \mathbf{v}_i(t) \cdot \mathbf{e}_{i,\ell}$ are the thermal particle fluctuations (with velocities $\mathbf{v}_i$) around their equilibrium positions projected onto the normal mode oscillation vectors $\mathbf{e}_{i,\ell}$ of mode ℓ.

The stability of the cluster is determined by the mode with the lowest eigenfrequency. It is thus very intriguing to study the lowest-frequency modes near the zigzag transition.

Starting with the experiment of anisotropy variation (by pressure variation) the frequency and oscillation patterns of the two lowest eigenmodes are shown in Fig. 5. (Actually, the lowest-frequency mode usually is the center-of-mass mode in y-direction at a frequency of $\omega_y = \sqrt{\beta}\omega_0$. Since this mode only reflects the external confinement and does not involve any relative particle motions it is irrelevant for the stability and is thus ignored.) At low pressure (and large parameter β) the lowest mode exhibits a preferred motion along the y-direction. The motion in x perpendicular to the chain is small. At higher pressure near the transition into the strict 1D chain a mode with decisive transverse activity takes over the role of the lowest frequency mode. These two modes are close in frequency and small in absolute value. The two mode patterns exactly reflect the competition be-

TABLE II. Scaling parameter r_0 and anisotropy parameter β determined from the observed configurations with $N=13$ at different gas pressures for a chosen value of $\kappa=0$ and $\kappa=1$.

$\kappa=0$	$p=4.0$ Pa	$p=4.9$ Pa	$p=6.0$ Pa	$p=6.8$ Pa
r_0/μm	490	430	390	370
$\beta/10^{-2}$	5.7	4.4	3.7	3.3
$\kappa=1$	$p=4.0$ Pa	$p=4.9$ Pa	$p=6.0$ Pa	$p=6.8$ Pa
r_0/μm	561	492	448	420
$\beta/10^{-2}$	2.9	2.3	2.0	1.8

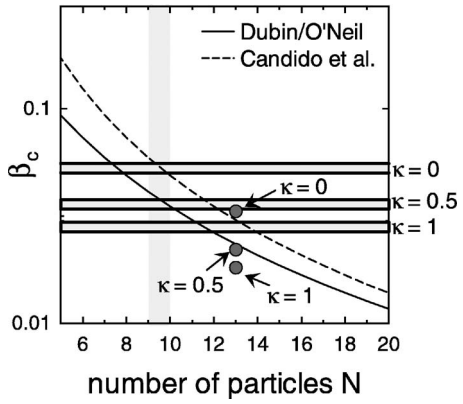

FIG. 4. Critical anisotropy parameter β as a function of particle number. The horizontal gray bars are the values of β determined from the experiment with particle number variation for different κ (compare Table I). The height of the bars indicate the rms errors of the experiment. The vertical gray bar indicates the region from $N=9$ to 10, where the zigzag transition occurs. The circles denote the β-values for $N=13$ of the experiment with gas pressure variation. The critical β is taken at the highest pressure where the zigzag pattern still is observed, i.e., at $p=6.8$ Pa. The solid and dashed line show the critical β from the models of Dubin and O'Neil [1] and Candido *et al.* [17], respectively.

tween the linear chain and zigzag configuration. Interestingly, this is still observable in the established zigzag configuration.

In turn, after the transition into the strict 1D chain (at 7.5 Pa) the lowest mode is one with pure transverse motion (in this case, the frequency of this mode is found to be

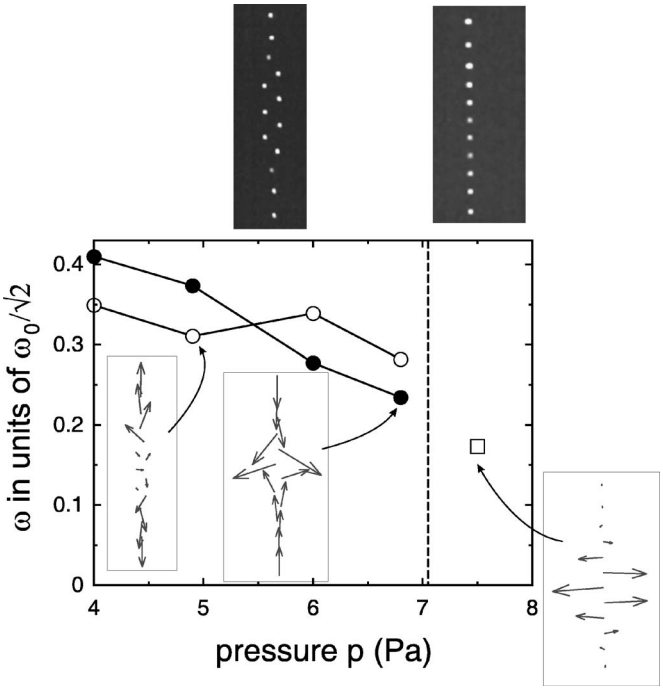

FIG. 5. Frequency of the lowest eigenmodes during pressure variation. The oscillation pattern of the corresponding eigenmodes is indicated in the insets. Below 7.5 Pa the cluster is in the zigzag state, above that pressure it forms a 1D chain.

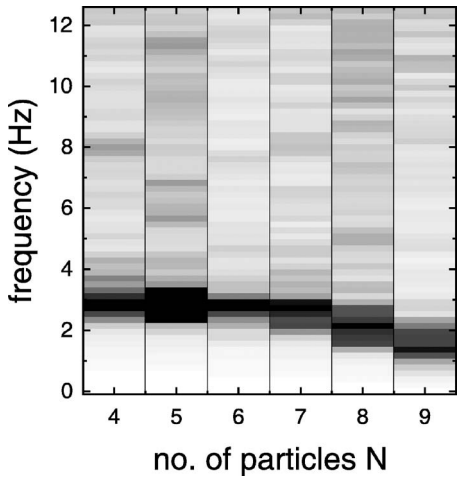

FIG. 6. Gray-scale plot of the spectral power density of the lowest perpendicular mode as a function of particle number in the cluster.

actually even smaller than that of the center-of-mass mode). The mode pattern obviously precisely reflects the tendency to form a zigzag pattern which is still visible in the linear chain configuration. The fact that this mode has such a low frequency shows that the 1D chain is very close to the zigzag transition. Thus, the dynamics directly reflect the static behavior of the cluster and contain information on the "other" side of the transition point.

This lowest-frequency transverse mode in the 1D chain will now be investigated for the linear chains with different particle number. This mode appears in the normal mode spectrum for each particle number that forms a strict 1D chain. Figure 6 shows the spectral power density of this transverse mode for the observed chains with particle numbers $N=4$ to 9. The maximum of the spectral power density is found at quite low frequencies below 3 Hz. It is easily seen that the maximum of the power density decreases with particle number, i.e., when approaching the zigzag transition at $N=10$. This substantiates the fact that this transverse mode is responsible for the stability of the cluster against the zigzag transition.

D. 1D modes

Finally, we like to investigate the normal modes of strict 1D linear chain configurations in longitudinal and transverse polarization. The $2N$ normal modes of a linear chain can be exactly divided into either motion purely along the linear chain (N longitudinal modes) or purely perpendicular to the chain (N transverse modes). For each longitudinal (transverse) mode, we have calculated the corresponding wave vector k. Here, the spatial Fourier components of the eigenvectors $\mathbf{e}_l^j$ ($\mathbf{e}_t^j$) of the longitudinal (transverse) modes along the chain are calculated from the relation

$$S_{l,t}(k) = \sum_{j=1}^{N} \mathbf{e}_{l,t}^j e^{iky_j}.$$

For example, the lowest frequency transverse mode with the alternating motion in Fig. 5 (at 7.5 Pa) would give a maxi-

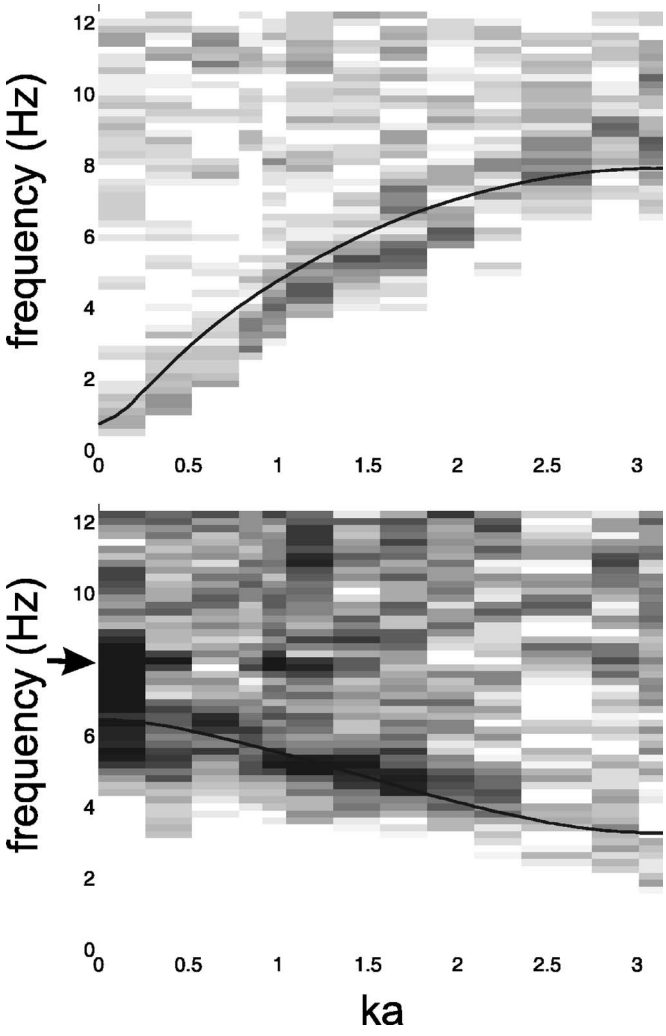

FIG. 7. Gray-scale plot of the spectral power density as a function of wave vector ka for the longitudinal (upper panel) and transverse (lower panel) modes. The solid line indicates the dispersion relation of the longitudinal and transverse wave in a linear chain according to Eq. (7) for $\kappa=0$. The high spectral activity at a frequency of 8 Hz in the transverse modes, as indicated by the arrow, is due to unwanted oscillations of the camera holder.

mum $S_t(k)$ at $k=\pi/a$ where $a=493$ μm is the interparticle distance.

From this, the dispersion relation of the longitudinal and transverse mode of a linear chain are derived: The spectral power density of each mode is plotted versus the wave vector ka as determined above. The dispersion relations are shown in Fig. 7 where the $N=13$ chain at $p=7.5$ Pa from the experiment with anisotropy variation has been analyzed. The longitudinal mode increases from small values to a maximum at $ka=\pi$. For long wavelengths $k\rightarrow 0$ the longitudinal mode goes to the very low-frequent center-of-mass mode in y-direction at the frequency $\omega_y=\sqrt{\beta}\omega_0$. The maximum at $ka=\pi$ is close to the dust plasma frequency ω_{pd} (see below).

In contrast, the transverse mode is an optical backward wave: The long wavelength limit is at $\omega_0=\omega_x$ and describes the center-of-mass mode in x-direction. The mode frequencies decrease for larger k. This corresponds to the fact that the lowest-frequency mode in Fig. 5 is one with alternating directions (corresponding to a wave vector of $ka=\pi$).

Similar dispersions of longitudinal waves have been studied experimentally and theoretically, e.g., by Refs. [10,11,20]. Also, the backward dispersion of transverse waves has been studied previously [11,21]. The observed longitudinal and transverse modes in this experiment are similar to investigations of Liu and Goree [11] who have studied the (driven and natural) phonon spectrum of 1D chains. The difference in our approach is that we have derived the dispersion from the determination of the normal modes whereas Liu and Goree have found the dispersion for any k directly from the particle motions without calculating of the normal modes. A similar attempt of deriving the dispersion from the normal modes has been followed for isotropic 2D clusters [22] where, however, the determination of the wave vectors from the mode patterns is more problematic.

Our measured dispersion is compared with the natural phonon spectrum

$$C(\omega,k)=\frac{\eta(\omega)}{m^2}\frac{\omega_{l,t}^2(k)}{(\omega^2-\omega_{l,t}^2(k))^2+\omega^2\nu^2} \tag{7}$$

as given by Liu and Goree [11]. Here, ν is the Epstein coefficient from friction with the neutral gas ($\nu\approx 7$ s^{-1} for our conditions) and $\omega_{l,t}^2(k)$ are the frequencies of the longitudinal and transverse mode at a wave vector k. These frequencies are given by [10,11,21,23]

$$\omega_l^2(k)=\beta\omega_0^2+w_{pd}^2\sum_{j=1}^{M}\frac{e^{-j\kappa}}{j^3}(2+2j\kappa+j^2\kappa^2)\sin^2\left(\frac{jka}{2}\right)$$

$$\omega_t^2(k)=\omega_0^2+w_{pd}^2\sum_{j=1}^{M}\frac{e^{-j\kappa}}{j^3}(1+j\kappa)\sin^2\left(\frac{jka}{2}\right),$$

where the dust plasma frequency

$$\omega_{pd}^2=\frac{Z^2e^2}{\pi\epsilon_0 ma^3}$$

defines the interaction strength. The parameter $\eta(\omega)$ is the spectral power density of a random force that mimics the excitation of natural phonons.

The natural phonon spectrum according to Eq. (7) contains the unknown quantities ω_0 and ω_{pd} which are determined by fitting the natural phonon model to the experimental power spectrum. A quite good agreement between the experimental normal mode dispersion and the natural phonons is obtained for $\kappa=0$. Thus, the normal mode analysis allows to retrieve the dispersion relation, again with a consistent value for κ. From the fit, the dust plasma frequency and the confinement are determined. The confinement frequency is obtained as $\omega_0/(2\pi)=6.5$ Hz and the dust plasma frequency is found as $\omega_{pd}=2.2\omega_0$.

From the fit value of the dust plasma frequency a dust charge of $Z=11\,300$ is derived. Instead of using the plasma frequency as a parameter describing the dynamics of the system the dust charge can also be determined from the static scale length r_0 [see Eq. (3)] from which a dust charge of $Z=11\,100$ is obtained. This is precisely in the range of charge

values as obtained in previous experiments on finite dust clusters under similar conditions [8].

IV. SUMMARY

To summarize, the zigzag transition of finite dust clusters has been analyzed experimentally. The zigzag transition has been driven by the increase of particle number or by the change of the anisotropy of the confinement by gas pressure variation. The observed transition points in particle number and anisotropy parameter are in very good agreement with simulation data for screening strengths between $\kappa=0$ and 1.

The dynamic stability of the system near the zigzag transition was analyzed and revealed that in the zigzag configuration the most unstable modes describe the competition between linear chain and zigzag configuration. In the strict 1D chain the lowest-frequency mode is a pure transverse mode with alternating motion. It precisely reflects the way the zigzag transitions develop. The modes thus contain the information of both sides of the transition.

The alternating transverse mode is found in all 1D chains. The mode frequency becomes smaller (and thus closer to the instability) when the particle number in the chain is increased and drops to zero at the zigzag transition which confirms the role of this mode during the transition.

Finally, the dispersion relation of the longitudinal and transverse modes in these linear chains has been derived from the normal mode spectra and is found to be in good agreement with the natural phonon spectrum in chains [11]. The dust charge obtained from the normal modes supports those obtained in isotropic 2D clusters [8].

The investigation of such transitions in the dimensionality of the clusters will allow much more sensitive measurements of the static and dynamic properties of Coulomb (Yukawa) clusters.

ACKNOWLEDGMENTS

This work is supported by the Deutsche Forschungsgemeinschaft via SFB-TR24 Grant No. A3.

[1] D. H. E. Dubin and T. M. O'Neill, Rev. Mod. Phys. **71**, 87 (1999).
[2] R. W. Hasse, Phys. Rev. Lett. **90**, 204801 (2003).
[3] P. Leiderer, W. Ebner, and V. B. Shikin, Surf. Sci. **113**, 405 (1982).
[4] R. Bubeck, C. Bechinger, S. Neser, and P. Leiderer, Phys. Rev. Lett. **82**, 3364 (1999).
[5] V. E. Fortov, A. V. Ivlev, S. A. Khrapak, A. G. Khrapak, and G. E. Morfill, Phys. Rep. **421**, 1 (2005).
[6] W.-T. Juan, Z.-H. Huang, J.-W. Hsu, Y.-J. Lai, and L. I, Phys. Rev. E **58**, R6947 (1998).
[7] M. Klindworth, A. Melzer, A. Piel, and V. A. Schweigert, Phys. Rev. B **61**, 8404 (2000).
[8] A. Melzer, Phys. Rev. E **67**, 016411 (2003).
[9] T. E. Sheridan, Phys. Rev. E **72**, 026405 (2005).
[10] A. Homann, A. Melzer, S. Peters, and A. Piel, Phys. Rev. E **56**, 7138 (1997).
[11] B. Liu and J. Goree, Phys. Rev. E **71**, 046410 (2005).
[12] O. Arp, D. Block, A. Piel, and A. Melzer, Phys. Rev. Lett. **93**, 165004 (2004).
[13] T. Antonova, B. M. Annaratone, D. D. Goldbeck, V. Yaroshenko, H. M. Thomas, and G. E. Morfill, AIP Conf. Proc. **799**, 299 (2005).
[14] O. Arp, D. Block, M. Klindworth, and A. Piel, Phys. Plasmas **12**, 122102 (2005).
[15] J. P. Schiffer, Phys. Rev. Lett. **70**, 818 (1993).
[16] H. Schollmeyer, A. Melzer, A. Homann, and A. Piel, Phys. Plasmas **6**, 2693 (1999).
[17] L. Candido, J.-P. Rino, N. Studart, and F. Peeters, J. Phys.: Condens. Matter **10**, 11627 (1998).
[18] S. Nunomura, J. Goree, S. Hu, X. Wang, A. Bhattacharjee, and K. Avinash, Phys. Rev. Lett. **89**, 035001 (2002).
[19] V. A. Schweigert and F. M. Peeters, Phys. Rev. B **51**, 7700 (1995).
[20] F. Melandsø and J. Goree, Phys. Rev. E **52**, 5312 (1995).
[21] T. Misawa, N. Ohno, K. Asono, M. Sawai, S. Takamura, and P. K. Kaw, Phys. Rev. Lett. **86**, 1219 (2001).
[22] A. Melzer, IEEE Trans. Plasma Sci. **32**, 594 (2004).
[23] F. Melandsø, Phys. Plasmas **3**, 3890 (1996).